Polarization conversion of excitonic photoluminescence under zero and nonzero magnetic fields in single InAlAs quantum dots

R. Kaji*, T. Shindo, S. Adachi, S. Muto

Department of Applied Physics, Hokkaido University, N13 W8, Kitaku, Sapporo 060-8628, Japan

Abstract

We demonstrated the circular to linear polarization conversion in single InAlAs/AlGaAs QDs. Since the anisotropic exchange interaction acts on the photo-created exciton spin as an in-plane effective magnetic field, the polarization of emissions can be converted from circular to linear and vice versa even under a zero external magnetic field. By using the quasi-resonant excitation, high conversion ratio up to ∼50% was obtained under nonzero longitudinal magnetic field. Additionally, exciton spin relaxation time and built-in linear dichroism were estimated by exciton spin dynamics in the 3D pseudospin precession model.

Key words: quantum dot, optical alignment, optical orientation, InAlAs, fine structure

1. Introduction

Dynamics of localized spins in the semiconductor quantum dots (QDs) are attractive from both fundamental and practical points of view. For the application to quantum information processing [1], as well as QD lasers and single-photon sources, the polarization of the emitted photon associated with the exciton annihilation is one of the key quantities. For ideal QDs, the eigenstates are bright excitons formed by the circularly polarized photon with the angular momentum ±1, and the polarization of the emission is detected as circularly polarized one (σ_+ or σ_-) via the selection rule of optical transitions. However, actual QDs contain the anisotropy of the shape and strain distribution originated from the QD formation process, and as a result, the confinement potential symmetry is reduced from D_{2d} to C_{2v} or lower. Since the anisotropic exchange interaction (AEI) caused by the symmetry reduction works as an in-plane magnetic field effectively, the precession of exciton spin with frequency $\Omega_{\rm exc} = \delta_{\rm b}/\hbar$ can be observed even under a zero external magnetic field. Here, $\delta_{\rm b}$ is the exciton fine structure splitting (FSS) and is of several tens μeV for typical InAlAs QDs. Consequently, AEI modifies the exciton eigenstates from $|\pm1\rangle$ to $|+1\rangle \pm |-1\rangle$, and at the recombination lifetime, the polarizations are converted to linear ones (x or y). In the sense that an exciton created with circularly polarized photon tends to emit the linearly polarized photon, this phenomenon can be interpreted as "polarization conversion". A lot of works related to similar conversion in the QD ensembles have already been reported so far (for example, for InAlAs/AlGaAs QDs [2] and CdSe/ZnSe QDs [3]). Yet, it is difficult to deduce the intrinsic parameters from ensemble average over QDs containing the inhomogeneous shape and strain distribution.

In this work, we demonstrate the polarization conversion for single InAlAs/AlGaAs QDs. The quasi-resonant excitation brings the high conversion efficiency under zero and nonzero longitudinal magnetic fields. Additionally, considering the exciton spin dynamics based on a simple coherent precession model permits us to estimate the exciton spin relaxation time and built-in linear dichroism.

2. Experiments

We used self-assembled $In_{0.75}Al_{0.25}As/Al_{0.3}Ga_{0.7}As$ QDs which were grown on a (100) GaAs substrate by molecular beam epitaxy [4]. Atomic force microscopy measurements on a reference, *i.e.* uncapped QD with the same growth conditions revealed that the average height and diameter of QDs are ∼4 and ∼20 nm with the areal QD density of $\sim 5 \times 10^{10}$ cm^{-2}. To perform the single QD spectroscopy, small mesa structures with typical diameter ∼150 nm were fabricated by wet etching and electron beam lithography.

A cw-Ti:Sapphire laser (∼1.664 eV) was used to illuminate the QD sample. As we shall see later, this photon energy corresponds to the quasi-resonant excitation for a target InAlAs QD. The photoluminescence (PL) signals were collected by an objective lens, and were detected with the triple-grating spectrometer (f=0.64 m) and the liquid nitrogen cooled Si-charge coupled device array. Though the energy resolution of our setup is ∼12 μeV, it can be improved to 5 μeV by the spectral fitting. The measurement temperature was kept to ∼5 K, and a magnetic field up to 5 T was applied in Faraday geometry ($\boldsymbol{B} \parallel \boldsymbol{k}$). The excitation polarization was fixed to σ_+ or σ_- by a quarter-wave plate and the polarization of PL spectra were analyzed with a half-wave plate (HWP) and a polarizer inserted in the detection path before the spectrometer.

*phone/fax: +81-11-706-6668
Email address: r-kaji@eng.hokudai.ac.jp (R. Kaji)

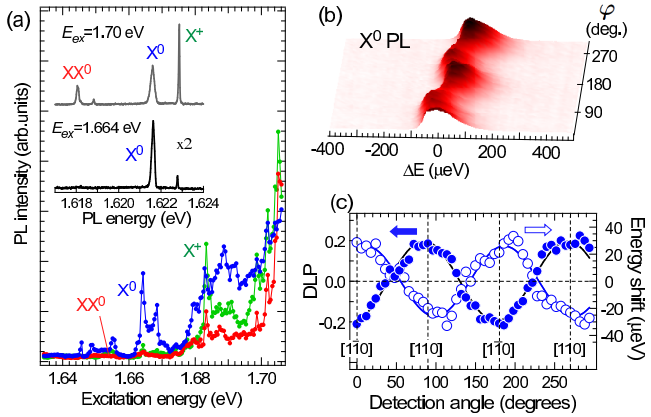

Figure 1: (a) The results of PL excitation spectra detected at the PL energies of X^0, X^+, and XX^0. Their charge states are assigned with a variety of measurements such as the exciton fine structure splitting, time-resolved recombination lifetime, and so on [8]. At the energy of 1.664 eV (~43 meV above the X^0 PL energy), X^0 PL is observed dominantly. (inset) PL spectra of the target single QD with wetting layer excitation (gray line) and quasi-resonant excitation (black). (b) 3D-plot of X^0 PL intensity. (c) Energy shift (open circles) and DLP (closed circles) under circularly polarized excitation. In both figures, the detection angle φ was used as a function.

3. Results and Discussion

3.1. Without magnetic field

To study the circular to linear polarization conversion, efficient generation and injection of bright excitons into their ground states are required. For this purpose, the excitation energy was tuned to 1LO resonance of the exciton ground state. As well known for InAlAs/AlGaAs QDs [2], CdSe/ZnSe QDs [3], InAs/GaAs QD [5], LO phonon-assisted excitation causes the fast energy relaxation of photo-created excitons with preserving the degree of spin polarization, and correspondingly is feasible for effective injection of the exciton with high spin polarization.

Fig. 1 (a) shows the time-integrated PL detected at the PL energy of neutral exciton (X^0), neutral biexciton (XX^0) and positively charged exciton (X^+) varying the excitation energy (E_{ex}) under a zero magnetic field. In the case of the wetting layer excitation (E_{ex} ~1.70 eV), as shown by the gray line in the inset, not only X^0 PL but XX^0 and X^+ can be observed simultaneously, and they decreased gradually with decrease of E_{ex}. At E_{ex} =1.664 eV (~745 nm), only X^0 indicates the abrupt increase (black line of the inset), which is identified as the LO phonon-assisted excitation. All of the experimental data shown hereafter were obtained with this excitation energy.

When the polarization of X^0 emissions was analyzed with a rotating HWP and a polarizer, not only the PL energy (Fig. 1 (c) open circles) but the intensity (Fig. 1 (b)) show the periodical changes under a circularly quasi-resonant excitation. In those figures, the detection angle φ was varied. The peak-to-peak amplitude of energy shift of ~50 μeV corresponds to the exciton fine structure splitting (δ_b), and the intensity modulation suggests the observation of the circular to linear (C→L) polarization conversion. In this paper, the degree of linear polarization (DLP) is used as a key index of the conversion efficiency, and defined as $\rho = \left(I_\varphi - I_{\varphi+\pi/2}\right) / \left(I_\varphi + I_{\varphi+\pi/2}\right)$. Here, $I_\varphi(I_{\varphi+\pi/2})$ is the PL intensity in the φ ($\varphi + \pi/2$)- frame. As shown in Fig. 1 (c), we observed the DLP of about 20% for X^0 PL under a zero magnetic field.

3.2. Model calculation

For more detailed analysis, we introduce the exciton pseudospin description. If we treat the bright exciton doublet $|\pm 1\rangle$ as an effective 3D pseudospin with $\boldsymbol{S}$=1/2, the exciton spin state can be depicted as a vector $\boldsymbol{S}$ in Bloch sphere. Additionally, the mutual conversion was considered between $\boldsymbol{S}$ and $\boldsymbol{\rho}$ which is a vector in Poincare sphere representing the light polarization. In this picture, the dynamics of the exciton spin (to be more exactly "pseudospin") is described by the following rate equation [3, 6],

$$\frac{\partial \boldsymbol{S}}{\partial t} = \boldsymbol{\Omega} \times \boldsymbol{S} - \frac{1}{\tau_s}\left(\boldsymbol{S} - \boldsymbol{P}_{\rm eq}\right) - \frac{1}{\tau_R}\left(\boldsymbol{S} - \boldsymbol{P}_{\rm ex}\right) \qquad (1)$$

where τ_s and τ_R are the exciton decay times caused by the spin relaxation and recombination, respectively. The vector $\boldsymbol{P}_{\rm ex} = (P_l, P_{l'}, P_c)$ is the excitation polarization vector in Poincare sphere, and is copied as the initial spin state in Bloch sphere. Here P_l and $P_{l'}$ are the DLP along [1$\bar{1}$0] and [100] crystallographic axes, and P_c is the degree of circular polarization (DCP: projection to [001]). The first term of the rhs of Eq. 1 represents the coherent spin precession induced by the effective field $\boldsymbol{\Omega}$, and second (third) term explains the decay of spin vector due to the exciton spin relaxation (recombination). Under a zero external field, the torque vector $\boldsymbol{\Omega}$ can be written as $\boldsymbol{\Omega} = (\Omega_{\rm exc}, 0, 0)$, and lies in the equatorial plane of the sphere. It is noteworthy that the polarization equilibrium $\boldsymbol{P}_{\rm eq} = (Y_l, 0, 0)$ is included in this model. Y_l leads to the convergence direction of $\boldsymbol{S}$ in xy-plane. Here, Y_l is used as a parameter of built-in linear dichroism of QD, and originates from the effects of valence-band mixing and thermalization. Although the main origin of Y_l has not been identified yet, this treatment brings a flexible way to the calculation. For simplicity, we assume that Y_l has the same sign with $\Omega_{\rm exc}$ and is in the [1$\bar{1}$0] axis. The information of steady state $\boldsymbol{S}$ is transferred to $\boldsymbol{\rho}$ when the exciton is recombined, and gives the polarization of the emission. By using the Stokes parameters ρ_l, $\rho_{l'}$ and ρ_c, which describe the DLP along [1$\bar{1}$0], [100] and the DCP, $\boldsymbol{\rho}$ can be written as $\boldsymbol{\rho} = (\rho_l, \rho_{l'}, \rho_c)$ where they satisfy the following relation; $|\boldsymbol{\rho}| = \sqrt{\rho_l^2 + \rho_{l'}^2 + \rho_c^2} \leq 1$.

From Eq. 1, the steady states of the polarizations can be derived as follows;

$$\rho_l = \left(\frac{Y_l}{\tau_s} + \frac{P_l}{\tau_R}\right) T_s \qquad (2)$$

$$\rho_{l'} = \frac{T_s}{\tau_R}\left[\frac{P_{l'}}{1 + (\Omega_{\rm exc} T_s)^2} - \frac{\Omega_{\rm exc} T_s P_c}{1 + (\Omega_{\rm exc} T_s)^2}\right] \qquad (3)$$

$$\rho_c = \frac{T_s}{\tau_R}\left[\frac{P_c}{1 + (\Omega_{\rm exc} T_s)^2} + \frac{\Omega_{\rm exc} T_s P_{l'}}{1 + (\Omega_{\rm exc} T_s)^2}\right] \qquad (4)$$

Here, T_s is the exciton spin lifetime and is represented as $T_s = \left(\tau_R^{-1} + \tau_s^{-1}\right)^{-1}$. As shown by Eqs. 3-4, the polarization

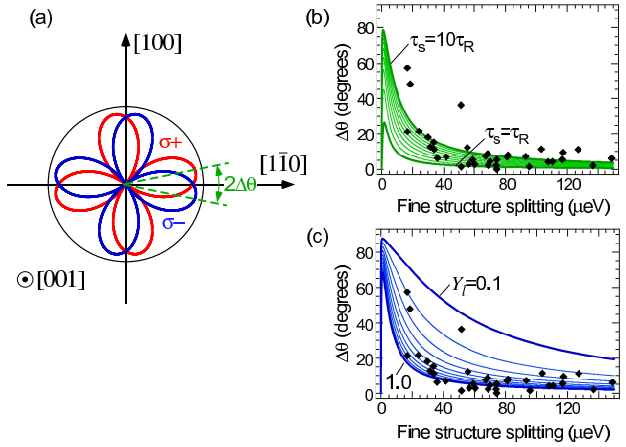

Figure 2: (a) Polar plot of the calculated DLP for σ_+ and σ_- polarized excitation. Depending on the the sign of P_c, polarization axis varies to $2\Delta\theta$. (b) and (c) δ_b-dependence of $\Delta\theta$ changing τ_s (b) and Y_l (c). By measuring $\Delta\theta$ for a number of InAlAs QDs with different δ_b, we can estimate τ_s ~$4\tau_R$ and Y_l ~0.5. Solid diamonds indicate the experimental data and curves show the calculation varying the τ_s/τ_R from 1 to 10 every 1 step (b) and Y_l from 0.1 to 1 every 0.1 step (c).

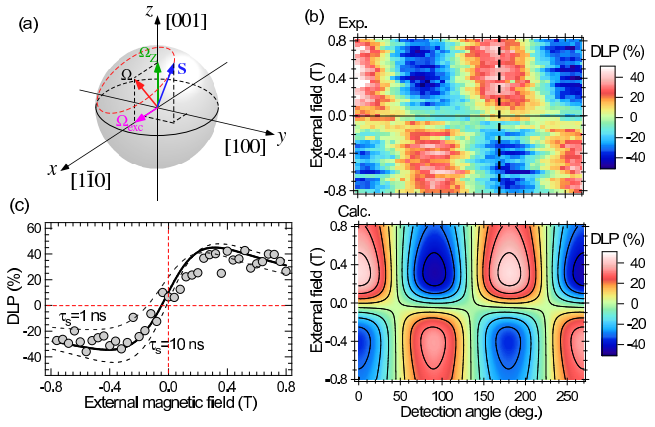

Figure 3: (a) Sketch of spin and torque vectors in Bloch sphere under longitudinal magnetic field. (b) Contour plot of C→L conversion for the target QD with δ_b =50 μeV and g_X =2.20; experimental results (upper panel) and calculated one (lower panel) as functions of B_z and φ. Other parameters used in the calculation are τ_R =0.75 ns, τ_s =3 ns, Y_l =0.5, respectively. (c) Cross-section curve at the dashed line in (b). At the external field $B_z \sim \delta_b/g_X\mu_B$, the maximum value of DLP was observed.

conversion from circular to linear ($P_c \rightarrow \rho_{l'}$) and vice versa ($P_{l'} \rightarrow \rho_c$) can be predicted. It should be noted that the observed DLP can be written as $\rho(\varphi) = \rho_l \cos(\varphi) + \rho_{l'} \sin(\varphi)$ in the laboratory frame.

Let us consider the phase difference of DLP depending on the excitation orientation. The initial spin states created by circularly polarized photons (σ_+, σ_-) are positioned at the poles of Bloch sphere. Though each vector starts the precession around $\mathbf{\Omega}$, the axes of observed DLPs are also symmetrical as for [1$\bar{1}$0] because both $\mathbf{\Omega}$ and Y_l distributions are directed to [1$\bar{1}$0] in our assumption. If the variation of DLP axis from [1$\bar{1}$0] is defined as $\Delta\theta$, the angle difference of $2\Delta\theta$ is observed from the σ_+ and σ_- excited DLP curves (Fig. 2 (a)). We measured the $\Delta\theta$ for a number of InAlAs QDs with the different FSS and plotted as a function of δ_b in Fig. 2 (b) and (c). In those figures, the calculated curves are depicted by changing τ_s/τ_R and Y_l, respectively. From both figures, it is shown that $\Delta\theta$ decreases with increasing δ_b. If a QD has a large δ_b, the spin vector precesses with a large angular frequency, and the steady state value comes close to Y_l regardless of the excitation polarization $\boldsymbol{P}_{ex}$. As a result, $\Delta\theta$ reduces with increasing δ_b. Compared with the calculation curves, the spin relaxation time of neutral exciton τ_s and the polarization equilibrium Y_l can be estimated roughly by using the recombination lifetime τ_R =0.75 ns, which is obtained by time-resolved PL measurements via a streak camera for a single InAlAs QD in the same sample. Since Y_l, τ_s, and τ_R may be different for individual QDs, dispersion from calculated curves is observed. However, many QDs are around the curve with τ_s ~$4\tau_R$, Y_l = 0.5, which are typical for average $In_{0.75}As_{0.25}As$ QDs. The obtained spin relaxation time agrees well with our previous results evaluated by the four-wave mixing technique for the same In/Al-ratio QD ensemble under a zero magnetic field (τ_s ~$5\tau_R$ [7]), and the photon correlation method for a single InAlAs QD (τ_s ~$3.6\tau_R$ [8]).

As seen in this section, the spin precession model and the introduction of Y_l offer a helpful way for the intuitive understanding of the exciton spin dynamics. However, high DLP under a zero magnetic field as shown in Fig. 1 (c) cannot be obtained only by the effect of Y_l. In order to explain this high DLP, we shall consider the effect of optically created nuclear field (B_N). As widely known, a continuous circular polarized excitation brings a non-zero magnitude of B_N, which works as an additional magnetic field along z-direction. With an effective formation of B_N via a positively charged exciton state by wetting layer excitation (*i.e.* non-resonant excitation), Belhadj *et al*. demonstrated the efficient polarization conversions under a zero magnetic field for single InAs QDs [9]. Although our experimental conditions (zero-magnetic field, quasi-resonant excitation) suppress large B_N formation, even a small B_N corresponding to the energy shift of ~5 μeV induces the observed high DLP [10]. More quantitative discussion will be seen elsewhere.

3.3. *Under longitudinal magnetic field*

In order to investigate the exciton spin dynamics more in detail and to achieve more efficient polarization conversion, similar experiments (that is, C→L conversion) under the longitudinal magnetic field B_z were performed for a typical single QD. B_z lifts the torque vector off the xy-plane $\mathbf{\Omega} = (\Omega_{exc}, 0, \Omega_Z)$ as shown in Fig. 3 (a). Ω_Z is the precessional frequency due to the Zeeman splitting, and written as $\Omega_Z = g_X\mu_B B_z/\hbar$, where g_X is the exciton g factor in growth direction and μ_B is Bohr magneton. For this InAlAs QD, g_X is found to be 2.20±0.01 by magneto-PL measurement under linearly polarized excitation. Fig. 3 (b) shows 2D-plot of DLP of X^0-PL as functions of B_z and φ (upper panel). Not only the DLP amplitude but its pattern is reproduced very well by the calculated shown in the lower panel. Here the following parameters were used; τ_R = 0.75 ns, τ_s =3 ns, and Y_l =0.5.

In addition, we shall consider the slant of DLP pattern observed in Fig. 3 (b). Compared with the calculated results, the angle at which maximum (or minimum) of DLP is detected is slightly tiled with respect to B_z. At the present stage, the effectively inclined magnetic field seems plausible candidate for the origin of this slant. If the sample growth axis and an external field $\boldsymbol{B}$ are not parallel for some technological reasons, in-plane component of the torque vector (Ω_x) changes its magnitude and direction depending on $\boldsymbol{B}$. Since the direction of Ω_x decides the polarization axis, the observed DLP pattern may be distorted by an effectively changing in-plane magnetic field. Though this slant pattern could be explained in the same model, more detailed discussion needs other experimental verification.

Let us focus on the profile (Fig. 3 (c)) at the dashed line in the 2D plot (Fig. 3 (b)). At $|B_z| \sim 0.35$ T, the DLP shows the maximum (minimum) when B_z was positive (negative). Zeeman splitting induced by this field has just the same energy of FSS (*i.e.* $\delta_b \sim g_X \mu_B B_z$), and the conversion efficiency reaches ~50%, which is the maximum value predicted by the above model (Eq. 1). Further increase of $|B_z|$ reduces the DLP amplitude, and this indicates the polarization of emitted light is close to circular. Since the magnetic confinement corrects the potential asymmetry, the effect of AEI will be diminished under a large magnetic field (~several Teslas). In addition, the amplitude of DLP is the asymmetric about $B_z = 0$ line. This can be explained by the effect of spin equilibrium Y_l. In the case of $B_z > 0$, the observed DLP (strictly speaking, ρ_l) increases from the initial value because $\boldsymbol{\Omega}$ (or $\boldsymbol{S}$) and Y_l are in the same half sphere ($x \geq 0$). However in the case $B_z < 0$, since $\boldsymbol{\Omega}$ directs oppositely and $\boldsymbol{S}$ precesses in the half sphere ($x \leq 0$) which does not contain Y_l, $\boldsymbol{S}$ is relaxed gradually into Y_l during the precession. Consequently, DLP becomes small. Though the precise evaluation of its magnitude is difficult, this fact implies Y_l has some finite value and can be estimated as ~0.5 for this target QD. The calculated results using $Y_l = 0.5$ and $\tau_R = 0.75$ ns, were obtained as shown by the solid curve in Fig. 3 (c), and τ_s is roughly estimated to be 3 ns. This is quite consistent with the estimation of $\tau_s \sim 4\tau_R$ obtained under a zero magnetic field.

4. Summary

In summary, the circular to linear polarization conversion was investigated for single InAlAs QDs under zero and nonzero magnetic fields. Quasi-resonant excitation made possible to inject the highly polarized exciton spin, and consequently the polarization conversion with high efficiency ~50% was achieved under a longitudinal magnetic field. Regarding the bright exciton doublets as two-level system, the dynamics was very well described by a simple rate equation which includes the spin equilibrium due to built-in linear dichroism. Measuring the angle difference of DLP or the conversion efficiency, Y_l and τ_s/τ_R were estimated. By using the recombination lifetime $\tau_R = 0.75$ ns which obtained by other independent measurement, we evaluated τ_s and Y_l as ~3 ns and 0.5, respectively for the target QD. The obtained τ_s under the magnetic fields was in good agreement with our results for the same InAlAs QD without a magnetic field. This long spin relaxation, exceeding the recombination lifetime, gives the valuable information on the aforementioned applications.

References

[1] D.D. Awschalom, N. Samarth, and D. Loss *Semiconductor Spintronics and Quantum Computation* (Springer, Berlin, 2002), Chap. 1.

[2] R. I. Dzhioev, B. P. Zakharchenya, E. L. Ivchenko, V. L. Korenev, Yu. G. Kusraev, N. N. Ledentsov, V. M. Ustinov, A. E. Zhukov, and A. F. Tsatsul'nikov, Phys. Sol. State **40**, 790 (1998).

[3] G.V. Astakhov, T. Kiessling, A.V. Platonov, T. Slobodskyy, S. Mahapatra, W. Ossau, G. Schmidt, K. Brunner, and L.W. Molenkamp, Phys. Rev. Lett. **96**, 027402 (2006).

[4] H. Sasakura, S. Adachi, S. Muto, H. Song, T. Miyazawa, and T. Usuki, Jpn. J. Appl. Phys. **43**, 2110 (2004).

[5] K. Kowalik, O. Krebs, A. Lemaitre, J. A. Gaj, and P. Voisin, Phys. Rev, B **77** 161305(R) (2008).

[6] E. L. Ivchenko, *Optical Spectroscopy of Semiconductor Nanostructures* (Alpha Science International Ltd., Harrow, UK, 2005).

[7] T. Watanuki, S. Adachi, H. Sasakura, and S. Muto, Appl. Phys. Lett. **86**, 063114/1-3 (2005).

[8] H. Kumano, S. Kimura, M. Endo, H. Sasakura, S. Adachi, S. Muto, and I. Suemune, J. Nanoelectron. Optoelectro. **1**, 39 (2006).

[9] T. Belhadj, C. M. Simon, T. Amand, P. Renucci, B. Chatel, O. Krebs, A. Lemaître, P. Voisin, X. Marie, and B. Urbaszek, Phys. Rev. Lett. **103**, 086601 (2009).

[10] R. Kaji, S. Adachi, T. Shindo, and S. Muto, Phys. Rev. B **80**, 235334 (2009).